MSW MANAGEMENT -Multidisciplinary, Scientific Work and Management Journal
ISSN: 1053-7899
Vol. 36 Issue 2, 2026, Pages 713-724

ADVANCES AND CHALLENGES IN UNDERSTANDING PIPELINE EROSION: INSIGHTS FROM EXPERIMENTAL AND COMPUTATIONAL STUDIES

Rahul Mishra[1], Roopesh Kumar Sinha[2*], Pankaj Sharma[3], Chandra Shekhar Verma[4], Sharda Pratap Shrivas[5], Vikky Kumhar[6]
[1]Department of Mechanical Engineering, Rungta International Skills University, Bhilai , Durg, Chhattisgarh 490024, India.
[2,3]Department of Mechanical Engineering, NMDC DAV Polytechnic Geedam Dantewada, Chhattisgarh 494441, India.
[4]Department of Basic Science (Physics) NMDC DAV Polytechnic Geedam Dantewada, Chhattisgarh 494441, India.
[5]Department of Mechanical Engineering, Chouksey Engineering College Bilaspur ,Bilaspur, Chhattisgarh 495004 India
[6]Department of Mechanical Engineering, Shri Shankaracharya Techcnical Campus, Bhilai, Durg ,Chhattisgarh 490020 , India
[*]corresponding Author Email- roopeshsinha12@gmail.com[2]
mishrarahul87@gmail.com[1], sharma7857@gmail.com[3], shekhar090677@gmail.com[4], pratapshrivas34@gmail.com, vikkykumhar@sstcc.in[6]

Abstract
Erosion caused by solid particles in pipelines is a persistent challenge across industries such as shale gas extraction, natural gas transportation, and pneumatic conveying systems. Critical components, including elbows, tees, and gate valves, are particularly vulnerable due to their complex geometries and exposure to turbulent flows. This review synthesises advancements in erosion research, highlighting the significant role of numerical simulation methods like Computational Fluid Dynamics (CFD) and Discrete Phase Models (DPM) in predicting erosion behaviour. Studies reveal that factors such as particle size, shape, impact angle, fluid velocity, and material properties strongly influence erosion rates, with elbows experiencing concentrated wear at downstream sections and gate valves showing high erosion near the sealing surface. Design modifications, including spiral pipelines, guide vanes, and erosion-resistant plates, have demonstrated their effectiveness in mitigating erosion. This review underscores the need for further research to optimise pipeline designs, improve predictive models, and ensure long-term system durability in challenging operational environments. Results indicate that erosion rates increase exponentially with fluid velocity, and reduced water content exacerbates material loss. Among the fittings analysed, blind tees exhibit better erosion resistance compared to elbows and right-angle pipes under certain conditions. The findings underscore the importance of selecting appropriate pipe components and controlling operational parameters to enhance pipeline longevity and ensure safety in shale gas transportation systems.

Key Words: *Hydrodynamic study, pressure drop, erosion prediction, two phase slurry flow, multiphase slurry flow, CFD, DPM*

Introduction

In this study, exhaustive review of existing literature has been done in order to investigate the erosion behaviour of three common pipeline fittings—90° elbows, right-angle pipes, and blind tees—under multiphase gas-liquid flow conditions. Among the most vulnerable components are elbows, tees, gate valves, and other fittings, where turbulent flows and secondary flow effects exacerbate wear and tear. Numerous studies have explored the factors contributing to pipeline erosion. Key determinants include particle characteristics such as size, shape, and hardness; fluid velocity and viscosity; and the material properties of the pipeline walls. Computational Fluid Dynamics (CFD) combined with numerical models such as Discrete Phase Models (DPM) and Discrete Element Methods (DEM) has emerged as a powerful tool to simulate erosion behaviour. These approaches enable researchers to predict erosion rates, analyse particle-wall interactions, and identify high-wear zones under varying operational conditions. Furthermore, innovative design solutions, such as spiral pipeline structures and erosion-resistant coatings, have been proposed to mitigate erosion and extend the lifespan of pipeline systems. Shale gas has emerged as a crucial energy source in the global drive towards cleaner and more sustainable energy systems. Compared to straight sections of pipelines, fittings such as elbows, tees, and blind tees are more susceptible to erosion due to their complex geometries. These structures tend to concentrate flow, increasing the likelihood of particle impacts and subsequent material wear. Consequently, understanding the erosion mechanisms in these critical components is essential to improving pipeline reliability and reducing maintenance costs. Erosion is influenced by various factors, including particle size, shape, and velocity, as well as fluid properties and pipe material characteristics. While experimental methods have provided valuable insights, numerical simulations using Computational Fluid Dynamics (CFD) have become increasingly popular for analysing erosion in complex multiphase flows. CFD techniques enable researchers to study the interaction between particles and pipe walls, providing detailed predictions of erosion rates under different conditions. Existing studies have primarily focused on straight pipes or standard elbow configurations, with limited exploration of more complex fittings like blind tees and right-angle pipes. Moreover, most research does not fully account for the operational conditions of shale gas fields, such as variations in water content and fluid velocity. Addressing these gaps is critical to developing more accurate models and designing erosion-resistant pipeline systems. This review synthesises key findings from experimental and numerical studies to provide a comprehensive understanding of erosion mechanisms in pipelines. By highlighting the challenges and advancements in the field, it aims to guide future research toward optimising pipeline designs and improving predictive models for long-term operational safety.

Literature Review

Hong. B. *et al.* (2023) studied that that solid particle erosion in pipelines has garnered significant attention, particularly in industries like shale gas production, where high-velocity flows and abrasive particles pose substantial challenges to pipeline integrity. This review synthesises the key advancements and gaps in understanding erosion phenomena, with a focus on pipeline components such as elbows, tees, and blind tees. The authors further explored that the Shale gas is a crucial energy resource, and its extraction often involves the transport of gas mixed with abrasive particles through pipelines. These particles, due to high-pressure differences and turbulent flow, cause significant wear on pipeline walls. Numerical methods like the Eulerian-Lagrangian and Discrete Phase Models (DPM) have been instrumental in modelling erosion. These approaches track particle trajectories and calculate their impact on walls based on flow characteristics. For instance, Yu *et al.* (2019) used CFD to examine the erosion behaviour of standard 90° elbows under gas-solid flows, while Kannojiya *et al.* (2018) focused on erosion in slurry flows. More recent studies by Ogunsesan *et al.* (2019) and Zhao *et al.* (2022) have expanded this research to include blind tees and valves, demonstrating the flexibility of CFD in adapting to different pipeline geometries. Complex pipe structures like elbows and tees experience higher erosion rates due to particle accumulation and turbulent flow patterns. For example, elbows tend to have concentrated erosion at the downstream outer wall, where particles collide with high velocity. Blind tees, however, show lower erosion rates in certain conditions because their geometry allows for energy dissipation and reduced particle velocities in plugged sections. Despite these findings, the literature lacks comprehensive studies on the erosion behaviour of tees and right-angled bends under realistic shale gas field conditions.While prior investigations have provided valuable insights, many studies have limitations. Most research focuses on simplified flow conditions or specific pipe components, without integrating the full complexity of field operations. Additionally, there is insufficient data on the role of fluid composition, such as varying water and gas content, in influencing erosion dynamics. Understanding these parameters is crucial for designing pipelines that are resilient to erosion over the lifecycle of a shale gas project. Building on existing knowledge, the reviewed paper uses advanced CFD-DPM methods to simulate the erosion of 90° elbows, right-angle pipes, and blind tees under multiphase gas-liquid flows. Yan. L. *et al*. (2024) numerically predicted the erosion rate of gate valve in gas solid flow. Gate valves are crucial control elements in pneumatic conveying systems, and impacts from solid particles frequently erode their sealing structures. Erosion causes the efficiency of the sealing to deteriorate and, in extreme situations, causes system failure. To solve this problem, a numerical model derived for a simplified two-dimensional gate valve, computational fluid dynamics (CFD) is created. The properties of gas-solid two-phase flow and erosion rate are examined using the two-way Euler-Lagrange method. By contrasting the simulation findings with experimental data, the simulation process is validated. The findings corroborates that the free shear layer above the cavity gets separated by the sealing surface which further creates a low velocity zone on it. The particles migrating at the downstream bottom surface are the main ones that have an impact on the sealing. The erosion data indicate that the top of the sealing surface has the highest rate of erosion. Additionally, the erosion rate in that area is decreased by the low-velocity zone. The authors further reviewed that CFD in conjunction with the Euler-Lagrange method was initially used by Abduljabbar et al. (2021) to investigate the effect of sandy flow on sand filter degradation. The McLaury model reduced the error in erosion results, according to the results of the numerical study. Based on a constructed semi-empirical erosion model, Tarodiya *et al.* (2022) employed the Computational Fluid Dynamics and Discrete Element Method (CFD-DEM) to investigate the erosion produced by sand-laden water flow on injectors. Dou *et al.* (2023) used the Computational Fluid Dynamics and Discrete Phase Model (CFD-DPM) method to gradually investigate the erosion behavior of solid particles on Weld Reinforcement Height. Beyralvand *et al.* (2023) examined the solid particle erosion in bent pipes with varying geometries using the CFD-DEM approach. Huang and colleagues (2024) used CFD-DPM method to study the motion of particle erosion inside the pipe bend. In order to investigate the wall erosion in a three-dimensional gate valve, Lin *et al.* (2014) used a two-way Eulerian-Lagrange approach based on CFD. The total erosion rate was created to quantify the degree of erosion. The CFD method was used by Peng *et al.* (2021) to investigate the erosion on the sealing surface of the ball valve under different operating

MSW MANAGEMENT -Multidisciplinary, Scientific Work and Management Journal
ISSN: 1053-7899
Vol. 36 Issue 2, 2026, Pages 713-724

circumstances. In conclusion, the primary reckoning techniques for researching attrition of particles are CFD-DEM and CFD-DPM. Particle flow within geometries is frequently simulated using the CFD-DEM approach. The author's further concluded that the repercussions of erosion qualities on the sealing facet and features of particle motion inside the gate valve are examined using the CFD-DPM approach, which entrenched the built CFD numerical model. According to erosion results, upper facet of sealing experience maximum erosion weighs up. The degree of gate valve opening causes an augmented erosion weigh up over the sealing facet. The maximal erosion rate is raised and its position is altered by both particle diameter and gas velocity. The erosion in the lowest section of the sealing facet is lessened by larger particle sizes. Wang. S. *et al.* (2022) numerically simulated the pipeline erosion due to sand particles is a critical issue in natural gas transportation systems, particularly in components like elbows and complex configurations. Sand-laden gas flows cause material degradation over time, risking pipeline integrity and operational safety. Computational Fluid Dynamics (CFD) has become a widely used tool to study erosion in pipelines. Coupled with Discrete Phase Models (DPM) or Discrete Element Models (DEM), CFD allows researchers to simulate the interaction of particles with the pipe wall. DPM is typically applied to dilute-phase flows, where particle-particle interactions are negligible, while DEM is more suited for dense-phase flows. For instance, Peng *et al.*(2016) developed predictive equations to identify maximum erosion locations in elbows, while Kosinska *et al.*(2020) analysed erosion rates for nano- and micro-sized particles. Their results indicated that particle size and velocity significantly impact erosion rates. Moreover, the influence of secondary flows and vortices, as noted in studies like those by Zeng *et al.*(2018), highlights the complexity of erosion in curved structures. Several optimisation strategies have been proposed to mitigate erosion in elbows. These include structural modifications, such as the addition of guide vanes or erosion-inhibiting plates, which alter flow characteristics to reduce wear. For example, studies by Li *et al.*(2022) demonstrated the effectiveness of design optimisation in reducing erosion through CFD simulations. Similarly, Farokhipour *et al.*(2019) suggested replacing standard elbows with plugged tees to improve erosion resistance. The findings reveal that the flow exiting the first elbow is not fully developed, causing irregular flow patterns and erosion in subsequent elbows. Studies like those by Zhang *et al.*(2018) and Wang *et al.*(2019) further explore the role of pipe orientation in affecting erosion rates. The orientation of pipelines, such as coplanar versus non-coplanar configurations, significantly influences particle trajectories and erosion distribution. While much progress has been made, gaps remain in understanding erosion behaviour under varying operational conditions. The researchers employed CFD-DPM methods to investigate erosion in π-shaped pipelines with different orientations. By comparing coplanar and non-coplanar configurations, this work aims to provide actionable insights into mitigating erosion through design improvements and operational adjustments.

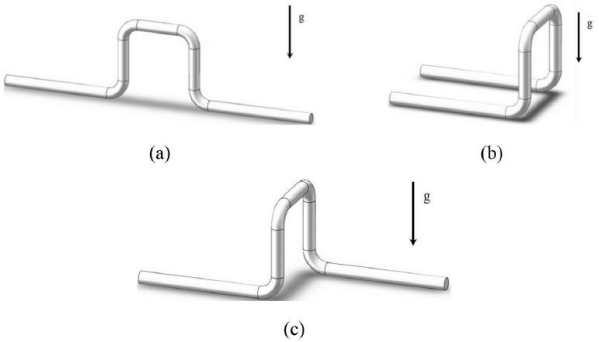

Figure. 1. The diagrammatic figures of the three π-shaped pipelines: (a) Structure-I; (b) Structure-II; (c) Structure-III.

It is very important to model the fluid domain before simulating erosion. Fig. 1 shows the illustrative representations of three distinct π-shaped pipeline orientations. Disparate pipe acclimatization was used to identify one coplanar pipeline and two non-coplanar pipelines. Their names were, Structure-I, Structure-II, and Structure-III, respectively. The accuracy of the erosion model was confirmed using experimental data from the literary texts Mazumder *et al.* (2008). The rate of erosion in ELBOW-1 at various axial points as determined by the imitation and the single data from the test was contrasted because the flow and erosion circumstances were identical. Table 1 lists the primary parameters that were employed in the experiment. The Finnie or DNV erosion models either overestimated or underestimated the size of the paramount attrition rate, as seen in Fig. 2. However, there was a satisfactory consensus between the Oka model's simulated findings along with the experimental evidence about the erosion trend and the erosion rate peak value. It is acceptable to overestimate the erosion rate between 25 and 45 degrees due to the imitation's unpredictability and the flow's intricacy. Thus, in further research, the Oka attrition model was applied.

Table 1. Dominant specification of the attrition test Mazumder *et al.* (2008)

Parameter	Value
Pipe inner diameter	25.4 mm
Curvature radius of elbow	38.1 mm
Pipe material	6061-T6 *Al*
Pipe density	2700 $kg \cdot m^{-3}$
Fluid	Air
Velocity	34.1 $m \cdot s^{-1}$
Mean diameter of particles	0.182 mm
Sand consumption	1.0 kg
Particle density	2600 $kg \cdot m^{-3}$
Run time	60 min

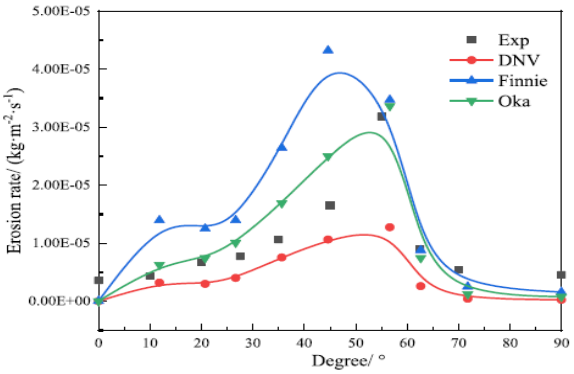

Figure.2. Collation of exploratory and imitated erosion values

MSW MANAGEMENT -Multidisciplinary, Scientific Work and Management Journal
ISSN: 1053-7899
Vol. 36 Issue 2, 2026, Pages 713-724

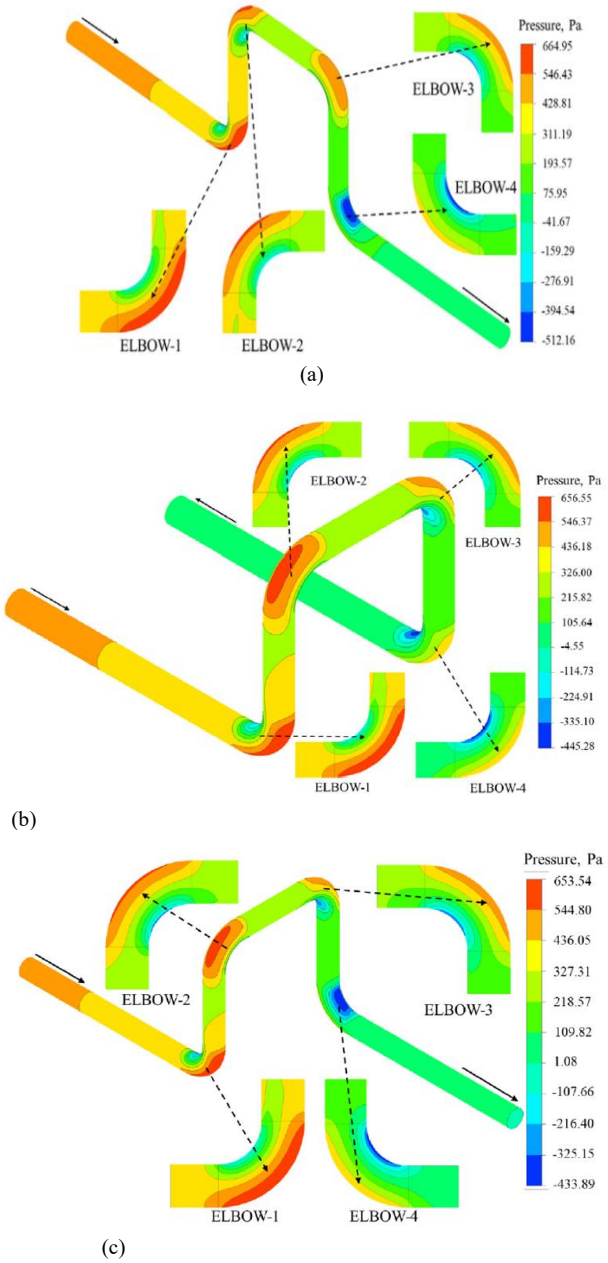

Figure.3. Pressure distribution in the three kinds of π-shaped pipelines: (a) Structure-I; (b) Structure-II; (c) Structure-III.

The distribution of pressure, velocity, and secondary flow in π-shaped pipelines was examined by Wang *et al.* (2022) in order to investigate the impact of changing the pipeline orientation on the flow field. The distribution of pressure Fig. 3 depicts the three π-shaped pipelines oriented differently. The authors concluded that Except at ELBOW-1, non-coplanar π-shaped pipes will cause fluids and particles to swirl. In ELBOW-2, an uneven and spiraling particle track was seen. ELBOW-4, and the spread of attrition clearly transposed. In non-coplanar structures, the paramount attrition rate of ELBOW-1–ELBOW-3 was constant, but in ELBOW-4, the combined effects of "pitting & swirling" or "cutting & swirling" caused a considerable change. In two non-coplanar structures, the inherent attrition rates of ELBOW-2 and ELBOW-4 rose by 72.49% and 87.48%, respectively, whereas ELBOW-3's integral erosion rate fell by 32.94%. The non-coplanar installation's swirling effect has a considerable and unavoidable aggravating influence on the inherent attrition extent of ELBOW-2 and ELBOW-4. In non-coplanar constructions, spiral particle clusters had a high-strength impact on the straight downstream pipe following ELBOW-4. On the pipe wall, a spiral erosion scar developed, and the paramount attrition rate was 1.20×10^{-6} $Kg.m^{-2}.S^{-2}$.

Dou. X. *et al.* (2023) had done CFD-DPM imitation of solid fragment attrition on weld augmentation height in liquid-solid high snip motion. In conveying and storage of oil and gas, liquid-solid two-phase flow attrition can result in significant financial losses as well as safety issues. By combining the computational fluid dynamics (CFD) and the solid particle attrition on weld reinforcement height (WRH) in liquid-solid high shear flows, the technique of the discrete phase model (DPM). The maximum attrition rates were considerably raised by the presence of flaws on the WRH surface. Slurry erosion and other liquid-solid two-phase flow erosion frequently affect pipelines Lin *et al.* (2014), hulls Liang *et al.* (2019), impellers, and pumps Dastkar *et al.* (2019), resulting in significant financial losses and safety issues Li *et al.* (2019) and Scheres *et al.* (2020). Regarding pipelines, the transportation and storage of oil and gas are negatively impacted by erosion wear brought on by solid particles. Solid particles will strike the pipeline facet as the particle-laden fluid passes through the pipelines, severing the facet metal and causing severe particle attrition due to inertia force Wang *et al.* (2022). Condensate washing-induced local corrosion failure has garnered more attention Yang *et al*. (2012) and Beccaria *et al.* (2013), particularly in the area of welded joints with noticeable electrochemical variations in pipelines. Each component of the welded joint has a varied composition, structure, and performance following the uneven heating and cooling process Chaves *et al.* (2011) and Zhao *et al.* (2016). As a result, the area of the welded connection is susceptible to cracks, porosity, and incomplete fusion. The flow rate and flow regime greatly influence the particle interactions in liquid-solid high shear flows because the solid particles can be effectively entrained by the liquid flow, particularly in high-viscosity liquids Ma *et al.* (2022). Regarding the pipeline surface, studies Elemuren *et al*. (2019) and Botros *et al*. (2018) have shown a positive correlation between erosion wear and solid particle concentration, and the "shielding effect" has been cited as the cause of the reduction in liquid-solid flow erosion at excessively high particle concentrations Macchini *et al*. (2013) and Anurag *et al*. (2020). Particle size has also been shown to have a substantial impact on erosion wear, aside from particle

MSW MANAGEMENT -Multidisciplinary, Scientific Work and Management Journal
ISSN: 1053-7899
Vol. 36 Issue 2, 2026, Pages 713-724

concentration, and larger particles are frequently associated with faster erosion rates Hattori *et al*. (2001). Extensive particles showed profound indentation depths, but small particles had extensive erosion regions, according to Stack *et al*.(2013).

The McLaury model Wang et al (2022) forecasted the rates of erosion. For the pressure-velocity coupling, the SIMPLE method was used. For the pressure interpolation, the conventional discretization techniques were used. Convective and divergent words were discretized using the QUICK technique. In order to increase computation accuracy, additionally, the roughness model, two-way coupling model, random track model, and grant rebound recovery model were used Li *et al.* (2022).

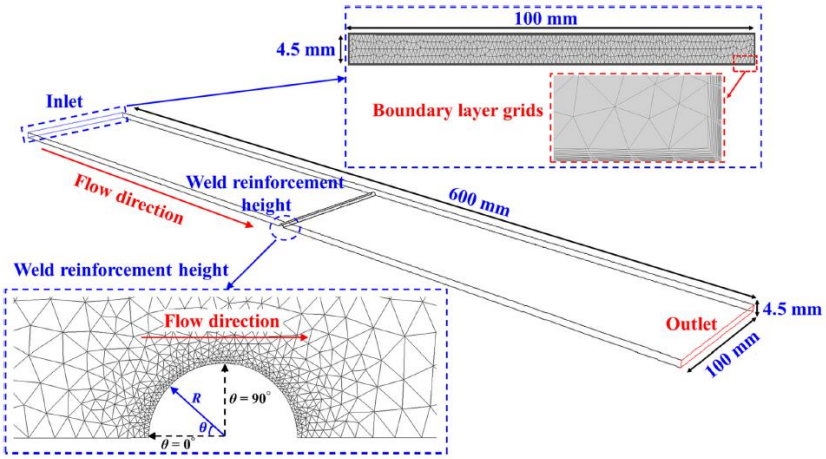

Figure.4. Computational domain geometry and meshes of the inlet and WRH.

Dou. X. *et al.* (2023) adopted McLaury model for speculating wall wear rate, as indicated in Eqs. (1)-(4).

$E = AV^n f(\gamma)$.....(1)

$A = FB_h^k$.....(2)

$f(\gamma) = b\gamma^2 + C\gamma\ \gamma < \gamma_{lim}$..... (3)

$f(\gamma) = xcos^2\gamma\sin(\omega\gamma) + \gamma sin^2\gamma + z\gamma > \gamma_{lim}$.....(4)

where f(γ) is the impact angle function, k is the erosion coefficient, B_h is the wall Brinell hardness, V is the particle impact velocity, and F is the empirical constant. Table 2 lists the empirical constants that were employed in the erosion model.

Constant	A	y	n	b	c	x	y	w
Value	1.44×10^{-8}	23°	2.1	−7	5.45	0.4	−0.9	−3.4

Table 2. Erosion model empirical constants

Huang. J. *et al.* (2024) numerically simulated particle erosion in 90-Degree elbow pipe of pneumatic conveying System. A novel comprehensive numerical model is proposed in this study to investigate the particle erosion behaviors (PEBs) in the 90-degree elbow pipe (90◦ EP) of the pigsty feed pneumatic conveying system (PFPCS) for gas–solid two phase flow (GSPF). Their method solves the particle tracking (PT) equation, pipeline heat transfer (PHT) equation, and Re-normalization group (RNG) k-ε problem using computational fluid dynamics and discrete phase modeling (CFD-DPM). It's interesting to note that this model improves the forecast accuracy of the erosion rate (η) by accounting for and verifying the thermophoretic force (FT), also known as the temperature effect. The η influence of several parameters, including the impact angle (θ), particle mass flow rate (m_p), and particle injection velocity (v), the particle shape factor (κp), the particle diameter (Dp), on the performance of 90◦ EP of PFPCS is then examined using this model. As a result, this research offers a conceptual foundation and a elevated entertainment analytical model for creating software for contemporaneous specifics conveyance that combines PFPCS components to create a health monitoring system. A number of pigsty feed technologies, including liquid feed conveying Kjeldager *et al.* (2021); Niederwerder *et al*. (2019), dry feed conveying Song *et al*. (2023); Wang *et al*. (2020), and pneumatic conveying Kong *et al.* (2022); Gomes *et al.* (2021), have been developed and implemented to date using a variety of principles and approaches. Longer conveying distance, higher conveying efficiency, higher levels of biosafety, and lower equipment maintenance costs are some of the advantages of pneumatic conveying over dry/liquid feed conveying methods in terms of particle erosion performance Lourenço *et al.* (2019). In particular, when high-speed feed travels through a turning section, the feed particles constantly affect the inner wall outside the 90◦ EP, causing significant erosion of the 90◦ EP, Yao *et al.* (2023); Liu *et al.* (2021); Xiao *et al.* (2021). Concurrently, this recurrent erosion may result in food safety incidents or pipeline damage Zang *et al.* (2023); Chen *et al*. (2023); Zhou *et al.* (2021). Actually, a number of factors affect the rate of erosion, making it challenging to determine the erosion distribution using an experimental approach Wang *et al*. (2020); Gu *et al*. (2022). Therefore, analytical imitations entrenched computational fluid dynamics (CFD) can be deployed for useful and affordable visual research techniques. In the meantime, the accurate attrition rate (η) observed in supplementary enterprises has not yet been matched by the relatively new application of CFD for particle attrition prophecy in pigsty feed pneumatic conveying systems (PFPCS).

The test geometry used in the research was a 90-degree elbow pipe (90◦ EP) of standard PCPI. Fig. 5 displays the 90◦ EP conceptual model and grid in PCPI. In order to accomplish conjunction of the partial differential equations (PDE) for computing the aforesaid multi physical field, COMSOL Multi physics 6.0, a rigorous calculation process, was installed. In particular, the discrete phase control equations (Eq. (5)) and gas phase control equations (Eqs. (6), (7), and (8)) are used to build the suggested model. MATLAB then computes the PDE, which consists of Eqs. (5), (6), and (8). In order to guarantee pressure-velocity coupling throughout the flow field computation procedure, the SIMPLE computing process was used. Additionally, Table 3 displays the physical characteristics of our suggested model that were employed in the computation. It also consults the structure parameters of universal PCPI, including FPC-80 (Qingdao Big Herdsman Co., Ltd.) and FPC-860 (Hangzhou Farm Intelligent Technology Co., Ltd.).

$\rho_a \frac{\partial u}{\partial t} + \rho_a \mathrm{u}.\nabla u = -\nabla p - f_D \frac{\rho_a}{2d_h} u|u| + F$.....(5)

$\frac{\partial A\rho_a}{\partial t} + \nabla.(A\rho_a u) = 0$.....(6)

The second component on the right-hand side of Eq. (5) can be used to represent the pressure drop, which is brought on by viscous shear. F is a volume force term, N/m^3, u is the fluid velocity, m/s, ρa is the fluid density, kg/m^3, p is the pressure, Pa, and dh is the mean hydraulic diameter, which may be written as dh = 4A/Z. Interestingly, A represents the cross section of 90◦ EP and can be written as A=πD_1^2. D_1 is the interior diameter of 90◦ EP, and Z is the wetted perimeter, m. Additionally, the Darcy friction factor in Eq. (5), which is a function of the Reynolds number (Re) and the surface roughness divided by the hydraulic diameter (e/d_h), represents the continuous pressure drop along the 90◦ EP segment. Interestingly, the unit tangent vector to the pipe axis is denoted by e. f_D (dimensionless) is described as follows:

$f_D = \frac{(1/1.8)^2}{(\log_{10}(\frac{e/d_h}{3.7})^{1.11} + (\frac{6.9}{Re}))^2}$.....(7)

The heat balance equation for the flow in 90º EP is expressed as follows:

MSW MANAGEMENT -Multidisciplinary, Scientific Work and Management Journal
ISSN: 1053-7899
Vol. 36 Issue 2, 2026, Pages 713-724

$$\rho_a AC_p \frac{\partial T}{\partial t} + \rho_a AC_p u.\nabla T = \nabla.Ak_a\nabla T + f_D \frac{\rho_a A}{2d_h}|u|^3 + Q + Q_{wall} \ldots\ldots\ldots(8)$$

where A is the 90◦ EP cross section, which can be written as A=πD_1^2, and ρa is the air density, kg/m3; T is the temperature, °C; ∇T is the temperature, °C·m^{-1}; and Cp is the heat capacity at constant pressure, J/(kg·K). Additionally, ka is the fluid's thermal conductivity, expressed as W/(m^2·K). Qwall denotes external heat exchange through the 90◦ EP wall, W/m; Q is a heat source, W/m. Since the calculated values of erosion rate (η) in all existing erosion models are statistically average, the statistics of particle number have a significant impact on the calculation results. According to Abuhatira *et al.* (2023), higher computation costs will provide larger particle numbers, but generally speaking, smaller particle number statistics result in less accurate calculation outputs. Therefore, an optimal particle number is highly efficient and economical for the calculated η. The calculated parameters of our model agree well with the experimental results. The accuracy and reasonableness of our model are confirmed in light of η_{max} & C_D based on the previously cited observations. The authors concluded that in earlier studies, the impact of ambient temperature on elbow erosion in 90◦ EP was disregarded, which led to a beneath model fidelity when collated to conceptual findings. As a more accurate, affordable, and non-invasive option to particle attrition prophecy and surveil, this study offers a novel ecumenical analytical model to examine the behaviors of particle attrition in 90◦ EP of the PFPCS. By adding FT to the GSPF's current PDE, CFDDPM models are put together and combined using FEA analysis to conduct η solution.

Table 3. Physical parameters of the proposed model

Parameters	Value
Fluid density ρ_a	1.29 kg/m^3
Fluid dynamic viscosity μ_a	17.9 × 10^{-6}Pa·s
Air inlet u	29.0 m/s
Coefficient of the fluid heat exchange k_a	0.023 W/(m^2·K)
The elbow Pipe density ρ_{ep}	2700 kg/m^3
Young's modulus of the pipe E_{ep}	70 GPa
Poisson's ratio of the pipe σ_{ep}	0.33
Coefficient of the pipe heat exchange k_{ep}	238 W/(m^2·K)
The inside diameter of the pipe D_1	80 mm
The outside diameter of the pipe D_0	85 mm
The radius of 90◦ elbow pipe R	200 mm
Density of the feed particle ρ_p	630 kg/m^3
The acceleration of gravity g	9.8 m/s^2
the heat capacity C_p	900 J/(kg·K)
The particle thermal conductivity k_p	0.16 W/(m^2·K)
The diameter range of the feed particle D_p	50 μm ~ 1000 μm
The velocity range of the particle injection v	5.0 m/s ~ 50.0 m/s
The particle mass flow rate range m_p	2.5 × 10^{-1}kg·s^{-1} ~ 21.0 × 10^{-1}kg·s^{-1}
The particle shape factor range κ_p	0.2 ~ 1.0
The impact angle θ	0 rad ~ π/2 rad
The surface temperature range of the pipe T_{ext}	5℃ ~ 50℃

By comparing eight different types of earlier erosion models, this solution approach concludes that the computed findings are very close to the experimental values. Their findings demonstrate the accuracy and noteworthy benefits of the suggested paradigm. In the meantime, the computed results show that the ∇T is created from the interior to the exterior in a circular motion of the 90◦ EP turning section, which is in good agreement with the particle trajectory prediction phenomenon.

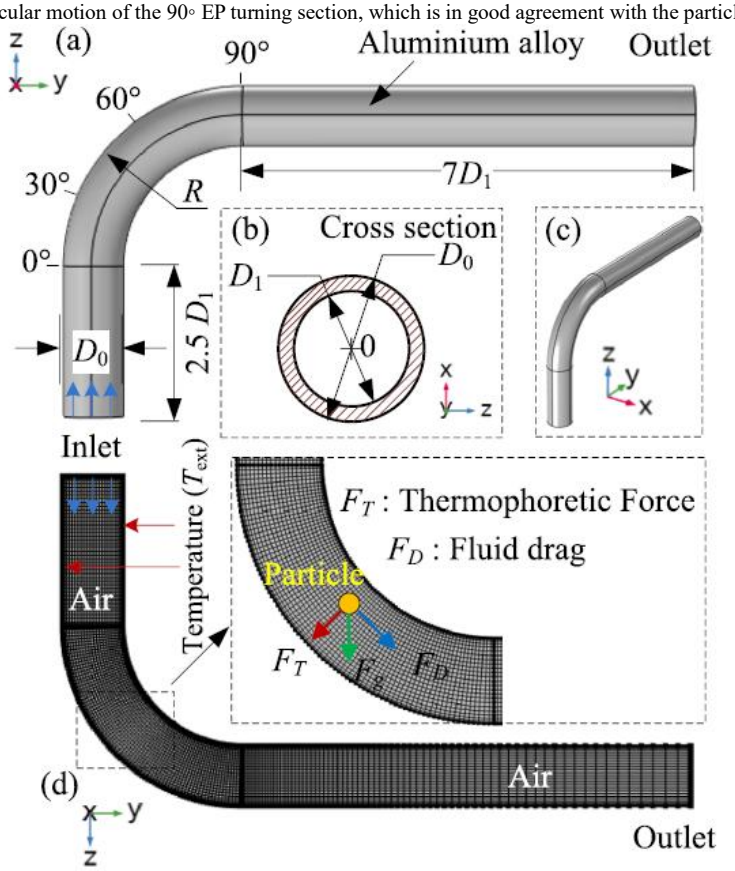

Figure.5. The geometric model and mesh of 90◦ EP in PCPI: (a) Schematic of the 90◦ EP in the y-z plane, (b) Schematic of the cross section of the 90◦ EP, (c) Schematic of the 90◦ EP, (d) The grid in FEA.

MSW MANAGEMENT -Multidisciplinary, Scientific Work and Management Journal
ISSN: 1053-7899
Vol. 36 Issue 2, 2026, Pages 713-724

Furthermore, using the temperature-regulated erosion model mentioned above, Software for monitoring the health of an aerial carrying pipeline may be created, offering a practical and affordable early prediction tool for usage in field livestock facilities.

Liu. E. Bin. *et al.* (2024) studied experimentally and numerically the attrition behaviour of the elbow of the meeting pipeline in shale gas field. The researchers observed that in the course of producing shale gas, the elbows of the meeting pipelines get seriously eroded because of prop pant flecks and rock spoilage which are induced conjointly. Earlier studies mainly focused on the influence of material and particle properties. For instance, Levy (1981) and Yabuki *et al.* (1999) explored material hardness and particle shape but lacked detailed analysis of impact angles. More advanced research, such as that by Yi *et al.* (2021), revealed distinct erosion mechanisms at varying impact angles, ranging from micro-cutting to plastic deformation. Experimental setups have been widely used to understand erosion mechanisms. Levy (1981) used blast testers to establish that material hardness inversely correlates with erosion rate. Nguyen *et al.* (2014) utilised wind and sand erosion testers to examine the effect of impact angles and exposure times on erosion characteristics. Khan *et al.* (2019) visualised erosion in elbow interiors using cut samples, highlighting the regions most prone to wear. While experiments have provided valuable insights, they often fail to capture the full complexity of real-world conditions, such as multiphase flows and dynamic operating environments. Sun and Cao (2021) highlighted the significance of particle-particle collisions on erosion rates, a factor often overlooked in earlier studies. Tofighian *et al*. (2020) demonstrated the importance of turbulence models in accurately predicting erosion patterns. The authors concluded that the elbow at various angles has distinct material removal mechanisms and erosion rates, according to the experimental results of gas-solid two-phase erosion Peng *et al.* (2021a), with the maximum erosion rate occurring at roughly 60º of the elbow. After numerically imitating the experimental pipe section and comparing the outcomes, it is discovered that the Oka model and the experimental data accord well. The relative error of the areas with high attrition rate is controlled within the range of approximately 11% to 18%, with high prophecy accuracy Peng *et al.* (2021b) and Qiao *et al*. (2021a). Additionally, the aforementioned parameters affect the area with the highest rate of erosion Qiao *et al.* (2021b). Following an exhaustive analysis of several variables, it was corroborated that the primary determinants of elbow attrition rate and attrition area dispensation are gas stream and particle accumulation extent. In order to lower the elbow's rate of erosion, this article suggests an inherent spiral tube anatomy. According to simulation research, the elbow's maximum attrition rate dropped by 11% and 34%, respectively, after the addition of the 1.2A and 1.5A spiral pipe sections in comparison to the pedestrian pipe sections. Table 4 displays the chemical composition of 20# carbon steel. The imitated functioning incidents are established based on the deployment site's on-site estimation, as indicated in Table 5.

Table 4. Chemical composition of 20# carbon steel

C	Si	Mn	S	P	Cr	Ni	Cu
17–0.24	17–0.37	0.35–0.65	≤0.35	≤0.035	≤0.25	≤0.25	≤0.25

Table 5. Imitation condition settings

Influence factors	Numerical simulation data
Gas flow rate, m/s	4, 6, 8, 10, 12, 14
Gathering pressure, MPa	4, 5, 6, 7, 8, 9
Particle size, mm	0.080, 0.096, 0.125, 0.150, 0.180, 0.212
Length of L1	20 D, 25 D, 30 D, 35 D
Gravity direction	+Y, −Y, +Z

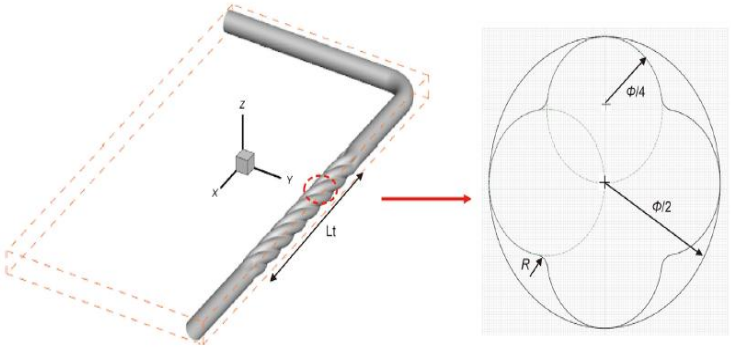

Figure.6. Schematic diagram of the spiral tube anatomy

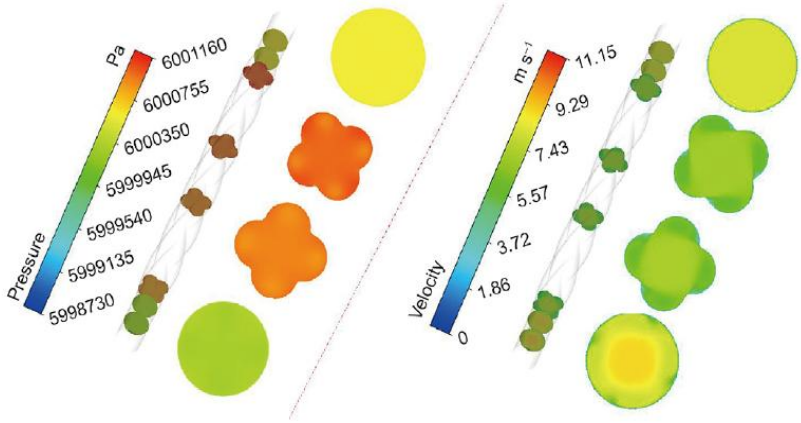

Figure.7. Cloud map of pressure and velocity of the spiral pipe

MSW MANAGEMENT -Multidisciplinary, Scientific Work and Management Journal
ISSN: 1053-7899
Vol. 36 Issue 2, 2026, Pages 713-724

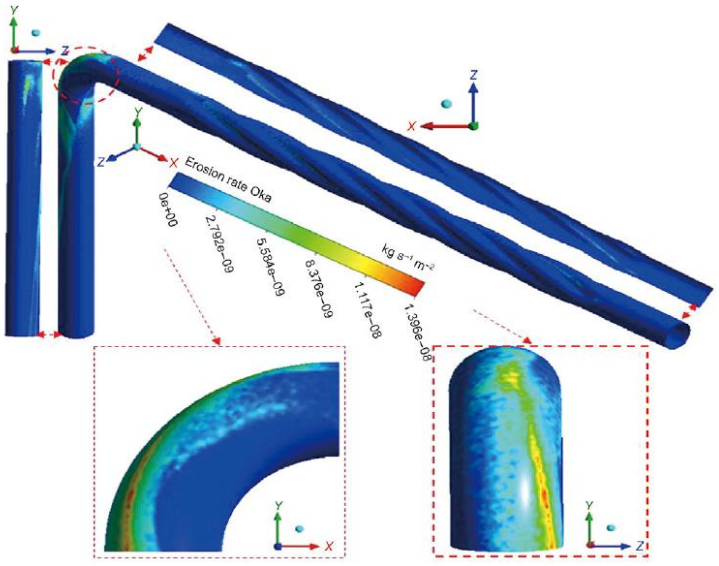

(a) 1.0A

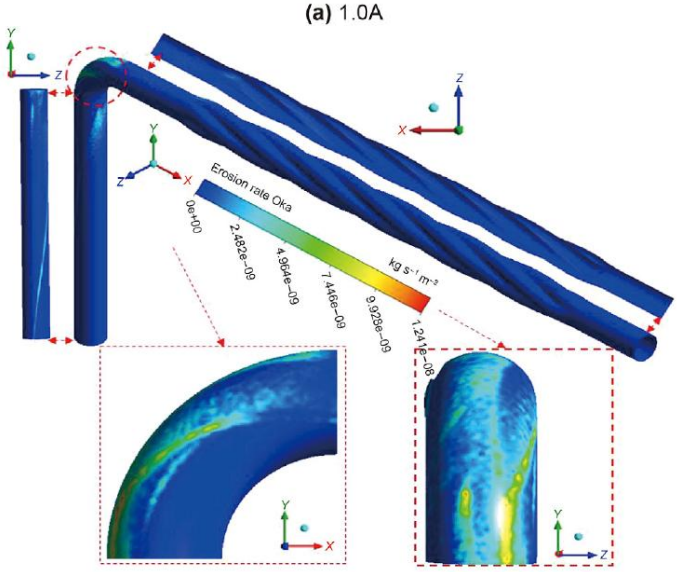

(b) 1.2A

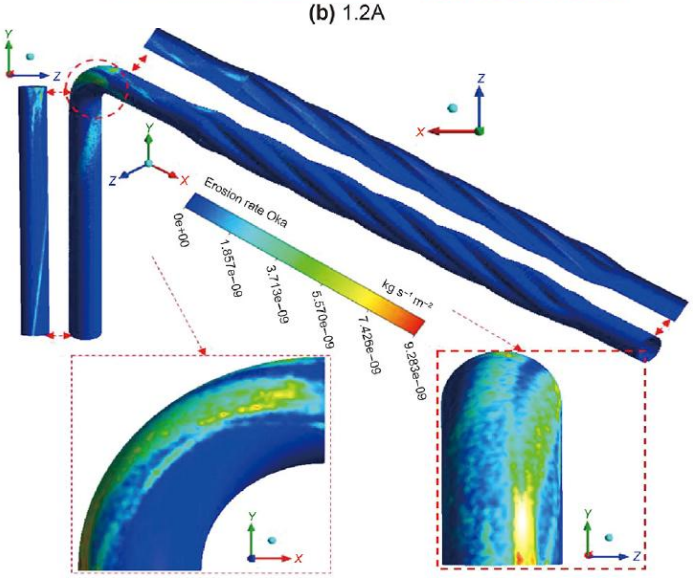

(c) 1.5A

Figure.8. Attrition cloud map of the spiral pipe

MSW MANAGEMENT -Multidisciplinary, Scientific Work and Management Journal
ISSN: 1053-7899
Vol. 36 Issue 2, 2026, Pages 713-724

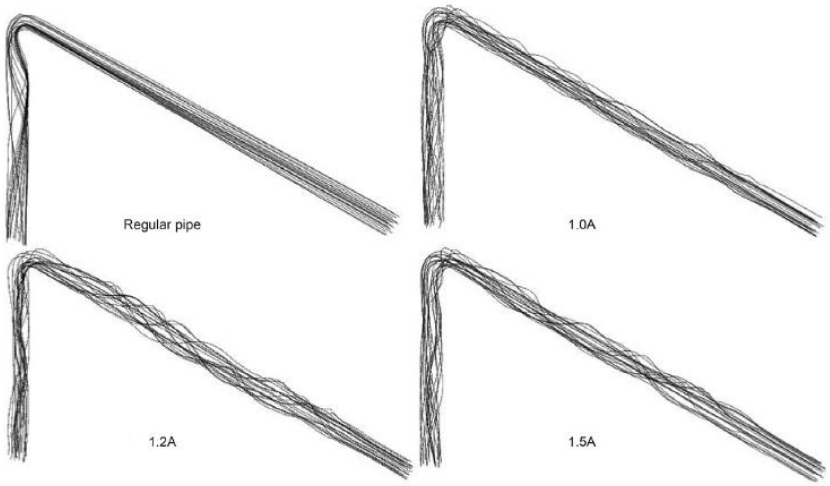

Figure.9. Particle trajectory diagram of the spiral pipe section

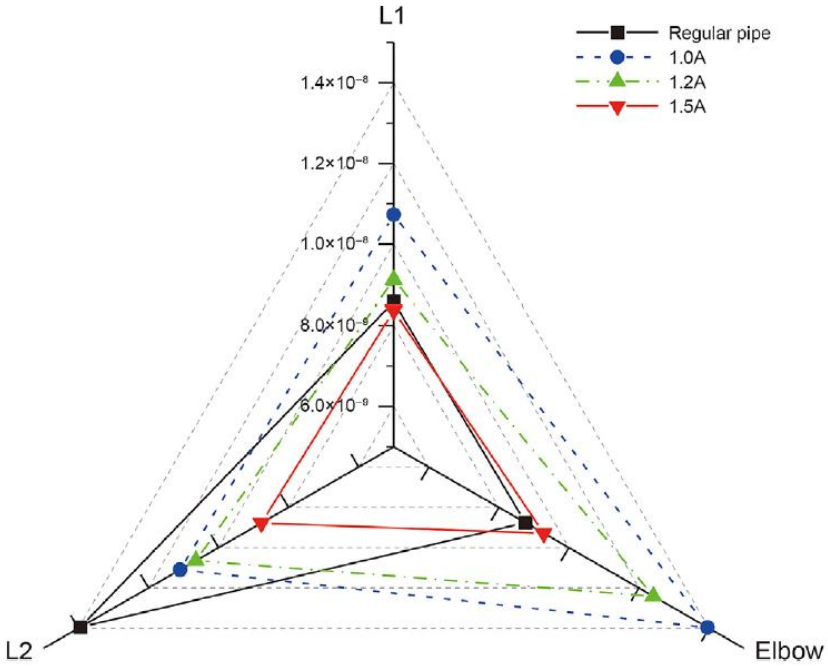

Figure.10. Erosion rate radar map of each part of the pipeline

The weightlessness method and scanning electron microscopy were used in this investigation to analyze the elbow's erosion rate and material removal mechanism, respectively. The attrition rate is calculated by the following formula:

$$ER = \frac{1}{3600000} \times \frac{w_0 - w_1}{S.t.\rho_w} \quad \text{.....(9)}$$

where t is the time the experiment was carried out, ρ_w is the density of the test piece material, S is the eroded area of the test piece surface, w_0 is the mass of the test piece prior to the experiment, and w_1 is the weight of the test piece following the experiment.

Model A and Model B are the two types of continuous phase controlling equations used in CFD. Of these, Model A holds that the pressure drop is the outcome of both gas and particle action, whereas Model B holds that the pressure drop is only influenced by gas movement. In this study, the gas-particle two-phase flow may be thought of as a simplified form of Model A. An encapsulation of Model A is as follows Parvaz *et al*. (2018):

Continuity equation:

$$\frac{\partial}{\partial t}\left(\varepsilon_g \rho_g\right) + \frac{\partial(\varepsilon_g \rho_g u_{g,i})}{\partial x_i} = 0 \quad \text{.....(10)}$$

Momentum conservation equation:

$$\frac{\partial}{\partial t}\left(\varepsilon_g \rho_g u_{g,i}\right) + \frac{\partial}{\partial x_j}\left(\varepsilon_g \rho_g u_{g,i} u_{g,j}\right) = -\varepsilon_g \frac{\partial p}{\partial x_i} + \frac{\partial}{\partial x_j}\left(\varepsilon_g \tau_{g,ij}\right) - S + \varepsilon_g \rho_g g_i \quad \text{.....(11)}$$

Where ε_g is the porosity; ρ_g is the gas density; p is the gas pressure; u_g is the gas velocity; τ_g is the gas viscosity; g_i is the acceleration of gravity; S is the momentum source term.

Haider and Levenspiel's (1989) force balance equation for discrete phase particles in the x direction in the Cartesian coordinate system looks like this:

$$\frac{du_p}{dt} = F_D\left(u - u_p\right) + \frac{g_x(\rho_p - \rho)}{\rho_p} + F_x \quad \text{.....(12)}$$

Where $F_D(u\text{-}u_p)$ is the drag force of particles per unit mass. F_D can be expressed as:

$$F_D = \frac{18\mu}{\rho_p d_p^2} \frac{C_D R_e}{24} \quad \text{.....(13)}$$

where m is the gas dynamic viscosity, r is the gas density, u is the gas flow rate, and up is the particle impact rate. Solid particle size is denoted by d_p, solid density by r_p, and the relative Reynolds number is denoted by Re., which is calculated by the following formula:

$$R_e = \frac{\rho d_p |u_p - u|}{\mu} \quad \text{.....(14)}$$

MSW MANAGEMENT -Multidisciplinary, Scientific Work and Management Journal
ISSN: 1053-7899
Vol. 36 Issue 2, 2026, Pages 713-724

C_D is the drag coefficient, and its expression is as follows:

$$C_D = a_1 + \frac{a_2}{R_e} + \frac{a_3}{R_e^2} \quad \text{.....(15)}$$

For spherical particles, within a certain range of Reynolds numbers, a_1; a_2; a_3 are constants (Jassim *et al*. 2010).

Duarte and Souza, (2017) suggested that an internal spiral tube shape that can be utilized for shale gas gathering. In contrast to earlier research, the structure's threads are situated on the pipe's inner wall surface, while the exterior wall facet is well ordered. This effectively controls the elbow erosion rate by increasing the flow area and decreasing the fluid flow rate in the pipe, as well as decreasing the intensity of particle accumulation by altering the direction of particle flow. As shown in Fig. 6, the elbow is positioned horizontally following a section of spiral pipe with a length of Lt=15 D. The spiral pipe section's flow area is $(2+\pi)\phi^2/8$, and the diameter of the common circumscribed circle is ϕ. Under the benchmark operating conditions, the spiral pipe's pressure and velocity cloud diagrams with 1.2 times the flow area is displayed in Fig. 7. It shows that the airflow velocity in the spiral pipe portion is between 6 and 7 m/s, which is far less than that in the traditional pipe, and that the highest-pressure difference is 2430 Pa. The erosion cloud diagrams for the 1.0A, 1.2A, and 1.5A spiral pipe sections are displayed in Fig. 8. It shows that the 1.0A, 1.2A, and 1.5A pipe sections have maximum rates of erosion of $1.396X10^{-8}$, $1.241X10^{-8}$, and $9.283X10^{-9}$ kg/(s.m^2), respectively, and that the elbow is where the areas with the highest rates of erosion are found. The standard pipe portion and the 1.0A pipe section have the paramount attrition rate. The maximum erosion rate of the 1.2A and 1.5A pipe sections is 11% and 34% lower, respectively, than that of the normal pipe segment. The particle trajectories of 1.0A, 1.2A, and 1.5A helical pipe sections and conventional pipe sections are devised in Fig. 9. It is clear that the addition of the spiral tube section considerably lessens the level of agglomeration of particles. The radar image of the attrition rate for three pipeline segments is displayed in Fig. 10. The traditional pipe section exhibits an acute triangle, as can be observed. The minimum angle of the triangle formed by 1.0A, 1.2A, and 1.5A on the radar chart steadily increases with the addition of the spiral pipe segment; thus, the pipeline's maximum erosion rate gradually falls. Because the triangle is almost equilateral at 1.5A and the maximum erosion rates of the three sections are equivalent, the spiral pipe section may reduce the maximum erosion rate of the entire pipeline, balance the gap between the erosion rates of L1 and L2 and the elbow, and improve pipeline safety.

Nemati. B. *et al.* (2024) using a distinct helical inner ring, the erosion decrease in elbows was explored numerically. As a new geometric idea for erosion management, the researchers offers a thorough numerical analysis of attrition in bends with inner rings. By employing accurate computational fluid dynamics (CFD) simulations, the CFD model used in this work includes the Grant and Tabakoff (1975) model to consider particle-wall collisions, the Oka model to simulate surface degradation, and the RNG k-ε turbulence model for flow solution. The investigation's main goal is to assess the various inner ring layouts' capacities to reduce erosion. According to the results, the elbow with two independent inner rings is an optimum design, showing a noteworthy 43% reduction in attrition when compared to the conventional elbow. Furthermore, the elbow with five distinct inner rings is a better option than the conventional elbow in accordance with the inherent attrition facet phenomenon. Furthermore, the study looks into how erosion is affected by an elbow with helical inner rings. This arrangement is seen to increase flow velocity, which speeds up particle motion and causes more erosion along the outer wall. According to studies, bends in pipes experience 50 times more erosion than straight pipelines. As a result, research into strategies to reduce erosion at bends is crucial Lin *et al.* (2015). Predictive models and correlation for elbow erosion have been developed as a result of extensive experimental study Finnie *et al.* (1960); Mazumder *et al.* (2008); Takahashi *et al.* (2010); Vieira *et al.* (2014). However, laboratory studies of three-dimensional erosion distribution are still difficult, and characterizing the three-dimensional erosion profile using ultrasonic transducers at different positions on the bend's outer surface is also difficult Peng *et al.* (2016). Computational fluid dynamics (CFD) numerical simulation is an effective method for erosion exploration. Three main steps are involved in the CFD-based erosion computation, which offers a thorough and comprehensive approach for precisely simulating erosion in a variety of intricate three-dimensional geometries: flow field modeling, particle trackingin the flow field and erosion rate calculation Arabnezad *et al*. (2015); Parsi *et al.* (2016). A vortex chamber can be added to reduce wear by increasing the cushioning effect and causing fluid rotation Duarte *et al.* (2016). They were aware, nevertheless, that persistent particle impacts might cause the materials being transported to deteriorate even more Duarte *et al.* (2017). The results show that the vortex chamber has a higher ability to reduce wear in situations with a high particle mass load, while the T-shaped tee is a superior option for diluted flows and low solid particle concentrations Duarte *et al.* (2020). Without altering the pipe volume, elbow wear can be decreased by joining a twisted strip inside the pipe Santos *et al*. (2016) or by constructing a twisted pipe upstream of the elbow in the direction of flow Duarte *et al*. (2017). Although they are difficult to construct and install, the two geometries mentioned above can extend the bend's usable life Li *et al*. (2022). Zhu and Li (2017) investigated numerically how a trapezoidal gear installed on a 90-degree elbow might reduce wear. The findings demonstrated the effectiveness of both single-row and multi-row protrusion configurations in lowering wear Li *et al*. (2022). To lessen erosion, Li *et al*. (2022) put up a guide vane downstream of a 90-degree elbow. They discovered that the guide vane's installation diminishes particle impact at the identical censorious point and gas velocity close to the outside wall Li. A. *et al.* (2022). The scattered phase is modeled in the Lagrangian reference frame observing the transport equations' solution for the continuous phase. The boundary conditions used is given in Table 6.

Table 6. Boundary conditions

Inlet boundary condition	velocity inlet	V = 34.1 m/s
Outlet boundary condition	pressure outlet	P = 0
Wall boundary condition	wall	No slip
Symmetry boundary condition	symmetry	

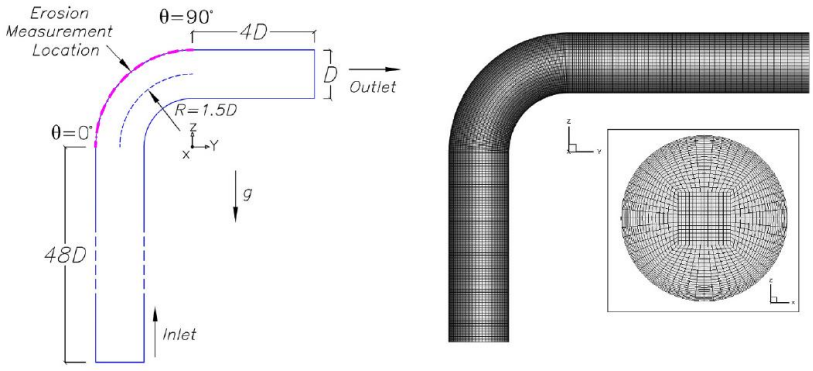

(a) General Geometry (b) Typical Meshed Domain

Figure.11. Schematic of the simulated validation case [Mazumder *et al.* (2008)]

The proposed erosion prediction equation by Oka *et al*. (2005) can be expressed as follows:

$$E(\alpha) = g(\alpha)E(90) \quad \text{.....(16)}$$

MSW MANAGEMENT -Multidisciplinary, Scientific Work and Management Journal
ISSN: 1053-7899
Vol. 36 Issue 2, 2026, Pages 713-724

The volume of eroded material per unit mass of impacting particles is represented by E(α) and E90 (mm^3/kg). E(α) represents the erosion at the particle's ideal impact angle, whereas E90 represents the erosion brought on by a typical impact. The particles' angular collision function, g(α), is determined by using two trigonometric functions in the manner shown below:

$$g(\alpha) = (Sin\alpha)^{n_1}(1 + Hv(1 - Sin\alpha))^{n_2} \quad \text{.....(17)}$$

The following equation uses the surface hardness, characteristics, and shape of the particles to determine the constant parameters n_1 and n_2:

$$n_1 n_2 = s(kv)^q \quad \text{.....(18)}$$

E90 is defined by the following equation and is dependent on the impact velocity, particle diameter, and surface hardness:

$$E90 = k(aHv)^{k_1 b}\left(\frac{u_p}{u_{ref}}\right)^{k_2}\left(\frac{D_p}{uD_{ref}}\right)^{k_3} \quad \text{.....(19)}$$

In this case, u stands for impact velocity (m/s) and D for particle diameter (μm). The standard impact velocity is called uref, while the standard particle diameter is called D_{ref}. The particle characteristics determine the coefficient k as well as the exponents k_1 and k_3. The material of the contacting surface and the particle characteristics dictate the exponent k_2:

$$k_2 = 2.3(Hv)^{0.038} \quad \text{.....(20)}$$

The contacting surface's Vickers hardness is indicated by the quantity Hv. The particle type and the hardness of the worn surface have a significant impact on the term $k(aHv)^{k_1 b}$. The link between the contacting surface's Vickers hardness and E90 in the standard impact velocity can be found using a function based on experimental data from Oka et al. (2005). The following function was determined in the research conducted by Santos *et al.* (2016):

$$k(aHv)^{k_1 b} \approx 81.714(Hv)^{-0.79} \quad \text{.....(21)}$$

Therefore, E90 can be expressed as follows:

$$E90 = 81.714(Hv)^{-0.79}\left(\frac{u_p}{u_{ref}}\right)^{k_2}\left(\frac{D_p}{uD_{ref}}\right)^{k_3} \quad \text{.....(22)}$$

By examining the kinetics of particle motion following collision, Grant and Tabakoff (1975) developed the particle rebound model. Based on experimental data on aluminum and sand in both normal and tangential directions to the wall, the following equations are given for the rebound coefficients of particles:

$$e_n = 0.993 - 1.76\alpha + 1.56\alpha^2 - 0.49\alpha^3 \quad \text{.....(23)}$$

$$e_t = 0.998 - 1.66\alpha + 2.11\alpha^2 - 0.67\alpha^3 \quad \text{.....(24)}$$

Another crucial element that needs to be taken into account in particle-wall interactions is friction. As stated in the preceding chapter, this investigation has employed FLUENT with a friction coefficient of μ = 0.35. It offers the best fit to the experimental findings, per the validation.

The influence of adding distinct, helical inner rings to a typical elbow in reducing erosion from particle impingement is the main topic of this paper, as illustrated in Fig. 12.

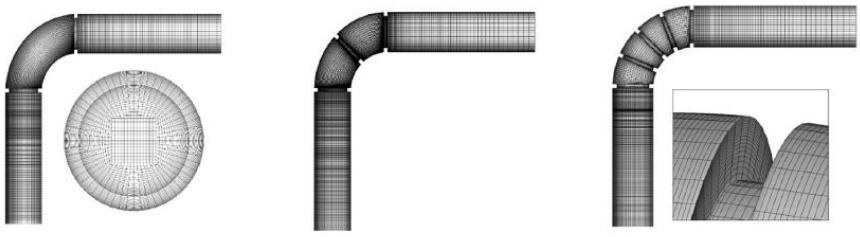

a) Elbow with 2 Inner Rings b) Elbow with 3 Inner Rings c) Elbow with 5 Inner Rings

Fig.12. Typical structural mesh used for elbows with separate inner rings.

CFD-DPM simulations were used in this study to investigate the anti-erosion properties of two geometric elbow models: helical and distinct inner rings. Prior to adding distinct inner rings and helical characteristics to the conventional geometry, the analytical imitation of the standard elbow was first verified using experimental data.

Scope of Work

The scope of this research focuses on investigating the erosion behaviour of pipeline components commonly used in industries like shale gas production and natural gas transportation. These components, including elbows, tees, and gate valves, are highly vulnerable to erosion due to their complex geometries and exposure to turbulent, high-velocity flows carrying solid particles.

This work aims to:

1. Analyse the factors influencing erosion, such as particle size, shape, impact angle, and fluid velocity, alongside material properties of the pipeline walls.
2. Apply advanced numerical simulation techniques, particularly Computational Fluid Dynamics (CFD) with Discrete Phase Models (DPM), to predict erosion patterns, identify high-risk zones, and evaluate erosion rates under realistic operating conditions.
3. Evaluate innovative mitigation strategies such as structural modifications (e.g., spiral pipeline structures, guide vanes) and erosion-resistant designs for critical components like elbows and gate valves.
4. Address the role of operational parameters like pipeline orientation, fluid composition, and flow dynamics in influencing erosion.
5. Propose design recommendations and predictive tools to optimise pipeline durability, reduce material loss, and enhance operational safety in real-world applications.

This study aims to provide actionable insights for designing erosion-resistant pipeline systems, with a strong emphasis on real-world conditions and operational sustainability.

Research Gap

Despite substantial advancements in understanding pipeline erosion, several critical gaps remain:

1. Most existing studies focus on simplified systems or specific pipeline components. The influence of field-specific parameters, such as varying gas and liquid compositions, multi-phase flow dynamics, and operational environments, remains underexplored.
2. While significant attention has been given to standard elbows, limited research exists on more intricate configurations, such as multi-elbow setups, blind tees, and π-shaped pipelines. Their erosion behaviours under realistic conditions need deeper investigation.
3. Few studies address the impact of pipeline orientation (e.g., coplanar vs non-coplanar setups) on erosion patterns, especially in series-mounted elbows and bends. Understanding these dynamics is critical for designing durable pipeline systems.
4. Though design solutions like spiral pipelines and erosion-resistant coatings have shown promise, their long-term effectiveness and adaptability under different operational conditions have not been extensively validated.
5. Current numerical models, including CFD-DPM and CFD-DEM, often rely on specific conditions and assumptions. Incorporating big data, machine learning, and artificial intelligence could significantly improve predictive accuracy and applicability to diverse field scenarios.

Addressing these research gaps is vital for advancing the understanding of erosion mechanisms, enhancing pipeline designs, and ensuring the long-term reliability of fluid transport systems in challenging industrial environments.

Conclusions

The study of erosion in pipelines has revealed that solid particle erosion poses a significant challenge to maintaining the integrity and efficiency of fluid transport systems, particularly in industries such as shale gas production and natural gas transportation. Key findings from the literature are summarised below:

MSW MANAGEMENT -Multidisciplinary, Scientific Work and Management Journal
ISSN: 1053-7899
Vol. 36 Issue 2, 2026, Pages 713-724

1. Pipeline components such as elbows, tees, and gate valves are the most vulnerable to erosion due to their complex geometries. Turbulent flows and secondary flow effects concentrate the impact of abrasive particles, resulting in higher erosion rates compared to straight pipeline sections. Elbows, for example, experience the most severe erosion at their downstream outer walls, while gate valves show maximum wear on their sealing surfaces, particularly at high gas velocities and smaller valve openings.
2. Erosion rates are heavily influenced by factors such as particle size, shape, hardness, impact velocity, and angle, as well as fluid properties like velocity and viscosity. Larger particles and higher velocities typically lead to more severe erosion, while fluid composition, such as gas-liquid ratios, also plays a critical role in determining erosion behaviour.
3. Numerical simulation methods, particularly Computational Fluid Dynamics (CFD) coupled with Discrete Phase Models (DPM), have proven to be powerful tools for predicting erosion patterns and identifying high-risk zones. These models enable detailed analysis of particle trajectories and wall impacts, with the Oka and McLaury models showing high accuracy in predicting erosion under specific conditions.
4. Various structural modifications have been proposed to mitigate erosion. Innovations such as spiral pipeline structures, erosion-resistant coatings, and the use of blind tees have demonstrated their effectiveness in reducing erosion by altering particle trajectories and dissipating energy. However, the long-term applicability of these solutions under real-world operational conditions requires further exploration.
5. Although significant progress has been made, there are notable gaps in understanding erosion under realistic field conditions. For example, the role of pipeline orientation (e.g., coplanar vs non-coplanar configurations) and the effect of multi-elbow setups have not been sufficiently explored. Additionally, integrating big data and machine learning into predictive models could enhance their accuracy and adaptability for diverse operational scenarios.
6. The findings suggest that optimising pipeline geometry and flow parameters, alongside implementing innovative mitigation strategies, can significantly reduce erosion risks. By adopting data-driven approaches and incorporating advanced simulation tools, industries can design more durable pipeline systems and extend their operational lifespan.

The literature highlights the importance of a multidisciplinary approach that combines experimental studies, numerical simulations, and innovative design strategies to address the persistent challenge of erosion in pipelines. While advancements in research have provided valuable insights, addressing the identified gaps is essential for ensuring long-term pipeline safety and efficiency in industrial operations.

References

Abduljabbar, A., Mohyaldinn, M., Younis, O., Alghurabi, A. (2021). A numerical CFD investigation of sand screen erosion in gas wells: effect of fine content and particle size distribution. J. Nat. Gas Sci. Eng. 95, 104228. https://doi.org/10.1016/j.jngse.2021.104228

Abuhatira, A.A., Salim, S.M., Vorstius, J.B. (2023). CFD–FEA based model to predict leak–points in a 90–degree pipe elbow. Engineering with Computers. https://doi.org/10.1007/ s00366-023-01853-4

Anurag, N., Mishra, S. Kumar. (2020). Slurry erosion: An overview. Materials Today: Proceedings 25, 659–663. https://doi.org/10.1016/j.matpr.2019.07.717

Arabnejad, H., Mansouri, A., Shirazi, S.A., McLaury, B.S. (2015). Development of mechanistic erosion equation for solid particles. Wear 332–333, 1044–1050. https://doi.org/10.1016/j.wear.2015.01.031.

Beccaria, A.M., Poggi, G., Castello, G. (2013). Influence of passive film composition and sea water pressure on resistance to localised corrosion of some stainless steels in sea water. Br. Corros. J. 30, 283–287. https://doi.org/10.1080/1478422X.2020.1866844

Beyralvand, D., Banazadeh, F., Moghaddas, R. (2023). Numerical investigation of novel geometric solutions for erosion problem of standard elbows in gas-solid flow using CFD-DEM. Res. Eng. Des. 17, 101014. https://doi.org/10.1016/j.rineng.2023.101014

Botros, K.K., Jensen, L., Foo, S. (2018), Determination of erosion-based maximum velocity limits in natural gas facilities. J. Natur. Gas Sci. Eng. 55, 395–405. https://doi.org/10.1016/j.jngse.2018.05.013

Chen, J., Cao, L., Song, G.B. (2023). Detection of the pipeline elbow erosion by percussion and deep learning. Mechanical Systems and Signal Processing 200 (11), 546–552. https://doi.org/10.1016/j.ymssp.2023.110546

Chaves, I.A., Melchers, R.E. (2011). Pitting corrosion in pipeline steel weld zones. Corros. Sci. 53, 4026–4032. https://doi.org/10.1016/j.corsci.2011.08.005

Dashtkar, A., Hadavinia, H., Sahinkaya, M.N., Williams, N.A., Vahid, S., Ismail, F., Turner, M. (2019). Rain erosion-resistant coatings for wind turbine blades: a review. Polym. Compos. 27, 443–475. https://doi.org/10.1177/0967391119848232

Dou, X., Xiang, W., Li, B., Ju, M., Li, A., Zhang, D., Li, Y. (2023). CFD-DPM modelling of solid particle erosion on weld reinforcement height in liquid-solid high shear flows. Powder Technol. 427, 118773. https://doi.org/ 0.3390/coatings13122080

Duarte, C.A.R., de Souza, F.J., dos Santos, V.F. (2016). Mitigating elbow erosion with a vortex chamber. Powder Technol. 288, 6–25. https://doi.org/10.1016/j.powtec.2015.10.032.

Duarte, C.A.R., de Souza, F.J. (2017). Innovative pipe wall design to mitigate elbow analysis. Wear 380–381, 176–190. https://doi.org/10.1016/j.wear.2017.03.015.

Duarte, C.A.R., de Souza, F.J., Venturi, D.N., Sommerfeld, M. (2020). A numerical assessment of two geometries for reducing elbow erosion. Particuology 49, 117–133. https://doi.org/10.1016/j.partic.2019.01.004.

Elemuren, R., Tamsaki, A., Evitts, R., Oguocha, I.N.A., Kennell, G., Gerspacher, R., Odeshi, A. (2019). Erosion-corrosion of 90◦ AISI 1018 steel elbows in potash slurry: effect of particle concentration on surface roughness. Wear 430-431, 37–49. https://doi.org/10.1016/j.wear.2019.04.014

Farokhipour, A., Mansoori, Z., Rasteh, A., Rasoulian, M.A., Saffar-Avval, M., Ahmadi, G. (2019). Study of erosion prediction of turbulent gas-solid flow in plugged tees via CFD-DEM. Powder Technol. 352, 136–150. https://doi.org/10.1016/j.powtec.2019.04.058

Finne, I. (1980). Erosion of surfaces by solid particles Oberfl¨achenerosion durch feste teilchen. Wear 3, 87–103. https://doi.org/10.1016/0043-1648(60)90055-7.

Gu, F.W., Zhao, Y.Q., Wu, F., Hu, Z.C., Shi, L.L. (2022). Simulation analysis and experimental validation of conveying device in uniform rrushed straw throwing and seed-sowing Machines using CFD-DEM coupled approach. Computers and Electronics in Agriculture 193 (10), 6720–6729. https://doi.org/10.1016/j.compag.2022.106720

Gomes, T.L.C., Lourenço, G.A., Ataíde, C.H., Duarte, C.R. (2021). Biomass feeding in a dilute pneumatic conveying system. Powder Technology 391, 321–333. https://doi.org/10.1016/j.powtec.2018.11.002

Grant, G., Tabakoff, W. (1975). Erosion prediction in turbomachinery resulting from environmental solid particles. J. Aircraft 12(5), 471–478. https://doi.org/ 10.2514/3.59826.

Haider, A., Levenspiel, O. (1989). Drag coefficient and terminal velocity of spherical and nonspherical particles. Powder Technol. 58 (1), 63-70. https://doi.org/10.1016/0032-5910(89)80008-7.

Hattori, S., Nakao, E. (2001). Cavitation erosion mechanisms and quantitative evaluation based on erosion particles. Wear 249, 839–845. https://doi.org/10.1016/S0043-1648(00)00308-2

Hong, B., Li, Y., Li, Y., Gong, J., Yu, Y., Huang, A., & Li, X. (2023). Numerical simulation of solid particle erosion in the gas-liquid flow of key pipe fittings in shale gas fields. Case Studies in Thermal Engineering, 42(November 2022). https://doi.org/10.1016/j.csite.2023.102742

Huang, J., Wen, J., Li, H., Xia, Y., Tan, S., Xiao, H., Duan, W., Hu, J. (2024). Particle erosion in 90-Degree elbow pipe of pneumatic conveying System: Simulation and validation. Comput. Electron. Agric. 216, 108534. https://doi.org/10.1016/j.compag.2023.108534

Jassim, E., Abdi, M.A., Muzychka, Y. (2010). A new approach to investigate hydrate deposition in gas-dominated flowlines. J. Nat. Gas Sci. Eng. 2 (4), 163-177. https://doi.org/10.1016/j.jngse.2010.05.005.

Kannojiya, V., Deshwal, M., Deshwal, D. (2018). Numerical analysis of solid particle erosion in pipe elbow. Mater. Today Proc. 5, 5021–5030. https://doi.org/ 10.1016/j.matpr.2017.12.080

Khan, R., Ya, H.H., Pao, W. (2019). An experimental study on the erosion-corrosion performance of AISI 1018 carbon steel and AISI 304L stainless steel 90-degree elbow pipe. Metals 9 (12), 1260. https://doi.org/10.3390/met9121260.

Kjeldager, C.K., Vodolazs'ka, D., Lauridsen, C., Canibe, N., Pedersen, L.J. (2021). Impact of supplemental liquid feed pre-weaning and piglet weaning age on feed intake post-weaning. Livestock Science 252 (10), 4680–4688. https://doi.org/10.1016/j.livsci.2021.104680

Kong, X.R., Liu, J., Yang, T.Y., Su, T.C., Geng, J., Niu, Z.Y. (2022). Numerical simulation of feed pellet breakage in pneumatic conveying. Biosystems Engineering 218, 31–42. https://doi.org/10.1016/j.biosystemseng.2022.03.012

Kosinska, A., Balakin, B.V., Kosinski, P. (2020). Theoretical analysis of erosion in elbows due to flows with nano-and micro-size particles. Powder Technol. 364, 484–493. https://doi.org/10.1016/j.powtec.2020.02.002

Li, A.J., Wang, Z.B., Zhu, L.Y., Wang, Z.L., Shi, J.Y., Yang, W.S. (2022). Design optimization of guide vane for mitigating elbow erosion using computational fluid dynamics and response surface methodology. Particuology. 63, 83–94. https://doi.org/10.1016/j. partic.2021.02.006.

Li, R., Sun, Z., Li, A., Li, Y., Wang, Z. (2022). Design optimization of hemispherical protrusion for mitigating elbow erosion via CFD-DPM. Powder Technol. 398, 117128. https://doi.org/10.1016/j.powtec.2022.117128.

Li, J., Sun, C., Shuang, S., Roostaei, M., Fattahpour, V., Mahmoudi, M., Zeng, H., Luo, J.- L. (2019). Investigation on the flow-induced corrosion and degradation behavior of underground J55 pipe in a water production well in the Athabasca oil sands reservoir. J. Pet. Sci. Eng. 182, 106325. https://doi.org/10.1016/j.petrol.2019.106325

Lin, C.H., Ferng, Y.M.. (2014). Predictions of hydrodynamic characteristics and corrosion rates using CFD in the piping systems of pressurized-water reactor power plant. Ann. Nucl. Energy 65, 214–222. https://doi.org/10.1016/j.anucene.2013.11.007

Lin, N., Lan, H., Xu, Y., Dong, S., Barber, G. (2015). Effect of the gas-solid two-phase flow velocity on elbow erosion. J. Nat. Gas Sci. Eng. 26, 581–586. https://doi.org/10.1016/j.jngse.2015.06.054.

Lin, Z., Ruan, X.-D., Zhu, Z.-C., Fu, X. (2014). Three-dimensional numerical investigation of solid particle erosion in gate valves. Proc. Inst. Mech. Eng. C J. Mech. Eng. Sci. 228 (10), 1670–1679. https://doi.org/ 10.1177/0954406213498543

Liu, E. Bin, Huang, S., Tian, D. C., Shi, L. M., Peng, S. B., & Zheng, H. (2024). Experimental and numerical simulation study on the erosion behavior of the elbow of gathering pipeline in shale gas field. Petroleum Science, 21(2), 1257–1274. https://doi.org/10.1016/j.petsci.2023.08.034

Liu, G.L., Ayello, F., Vera, J., Eckert, R., Bhat, P. (2021). An exploration on the machine learning approaches to determine the erosion rates for liquid hydrocarbon transmission pipelines towards safer and cleaner transportations. Journal of Cleaner Production 295 (12), 6478–6487. https://doi.org/10.1016/j.jclepro.2021.126478

Levy, A.V. (1981). The solid particle erosion behavior of steel as a function of microstructure. Wear 68 (3), 269-287. https://doi.org/10.1016/0043-1648(81)90177-0.

MSW MANAGEMENT -Multidisciplinary, Scientific Work and Management Journal
ISSN: 1053-7899
Vol. 36 Issue 2, 2026, Pages 713-724

Liang, L., Pang, Y., Tang, Y., Zhang, H., Liu, H., Liu, Y. (2019). Combined wear of slurry erosion, cavitation erosion, and corrosion on the simulated ship surface. Adv. Mechan. Eng. 11, 1687814019834450. https://doi.org/10.1177/1687814019834450
Lourenço, G.A., Gomes, T.L.C., Duarte, C.R., Ataíde, C.H. (2019). Experimental study of efficiency in pneumatic conveying system's feeding rate. Powder Technology 343, 262–269. https://doi.org/10.1016/j.powtec.2018.11.002
Ma, X.G., Yang, X.D., Hu, H.X., Zheng, Y.G. (2022). Numerical simulation of particle concentration and size on the slurry erosion on the surface of V-shaped groove microstructure. J. Korean Phys. Soc. 80, 991–1002. https://doi.org/10.1007/s40042-022-00462-6
Macchini, R., Bradley, M.S.A., Deng, T. (2013). Influence of particle size, density, particle concentration on bend erosive wear in pneumatic conveyors. Wear 303, 21–29. https://doi.org/10.1016/j.wear.2013.02.014
Mazumder, Q.H., Shirazi, S.A., Mclaury, B. (2008). Experimental investigation of the location of maximum erosive wear damage in elbows. J. Press. Vessel. Technol. 130(1), 011303. https://doi.org/10.1115/1.2826426
Nemati, B., Vaghefi, M., & Behroozi, A. M. (2024). Numerical investigation of the erosion reduction in elbows using separate and helical inner ring. Results in Engineering, 23(March), 102499. https://doi.org/10.1016/j.rineng.2024.102499
Nguyen, Q.B., Nguyen, V.B., Lim, C.Y.H., et al. (2014). Effect of impact angle and testing time on erosion of stainless steel at higher velocities. Wear 321, 87-93. https://doi.org/10.1016/j.wear.2014.10.010.
Niederwerder, M.C., Stoian, A., Rowland, R., Dritz, S.S., Petrovan, V., Constance, L.A., Hefley, T.J. (2019). Infectious dose of african swine fever virus when consumed naturally in liquid or feed. Emerging Infectious Diseases 25 (5), 891–897. https://doi.org/10.3201/eid2505.181495
Ogunsesan, O.A., Hossain, M., Iyi, D., Dhroubi, M.G., Abdel Wahab, M. (2019). CFD Modelling of Pipe Erosion Due to Sand Transport BT. Proceedings of the 1st International Conference on Numerical Modelling in Engineering, Springer Singapore, Singapore, 274–289.
Oka, Y.I., Okamura, K., Yoshida, T. (2005). Practical estimation of erosion damage caused by solid particle impact: Part 1: effects of impact parameters on a predictive equation. Wear 259, (1–6), 95–101. https://doi.org/10.1016/j. wear.2005.01.039.
Oka, Y.I., Yoshida, T. (2005). Practical estimation of erosion damage caused by solid particle impact: Part 2: mechanical properties of materials directly associated with erosion damage. Wear 259(1–6), 102–109. https://doi.org/10.1016/j. wear.2005.01.040.
Parsi, M., Kara, M., Kesana, N., Jatale, A., Shirazi, S. (2016). CFD simulation of sand particle erosion under multiphase flow conditions. Wear 376–377, 1176–1184. https://doi.org/10.1016/j.wear.2016.12.021.
Parvaz, F., Hosseini, S.H., Elsayed, K., et al. (2018). Numerical investigation of effects of inner cone on flow field, performance and erosion rate of cyclone separators. Separ. Purif. Technol. 201, 223-237. https://doi.org/10.1016/j.seppur.2018.03.001.
Peng, D., Dong, S., Wang, Z., Wang, D., Chen, Y., Zhang, L. (2021). Characterization of the solid particle erosion of the sealing surface materials of a ball valve. Metals 11 (2), 263. https://doi.org/10.3390/met11020263
Peng, S., Chen, R., Yu, B., et al. (2021a). Daily natural gas load forecasting based on the combination of long short term memory, local mean decomposition, and wavelet threshold denoising algorithm. J. Nat. Gas Sci. Eng. 95, 104175. https://doi.org/10.1016/j.jngse.2021.104175.
Peng, S., Zhang, Z., Liu, E., et al. (2021b). A new hybrid algorithm model for prediction of internal corrosion rate of multiphase pipeline. J. Nat. Gas Sci. Eng. 85, 103716. https://doi.org/10.1016/j.jngse.2020.103716.
Peng, W., Cao, X. (2016). Numerical simulation of solid particle erosion in pipe bends for liquid-solid flow. Powder Technol. 294, 266–279. https://doi.org/10.1016/j.powtec.2016.02.030.
Peng, W.S., Cao, X.W. (2016). Numerical prediction of erosion distributions and solid particle trajectories in elbows for gas solid flow. J. Nat. Gas Sci. Eng. 30, 455–470. https://doi.org/10.1016/j.jngse.2016.02.008
Qiao, W., Liu, W., Liu, E. (2021a). A combination model based on wavelet transform for predicting the difference between monthly natural gas production and consumption of US. Energy 235, 121216. https://doi.org/10.1016/j.energy.2021.121216.
Qiao, W., Wang, Y., Zhang, J., et al. (2021b). An innovative coupled model in view of wavelet transform for predicting short-term PM10 concentration. J. Environ. Manag. 289, 112438. https://doi.org/10.1016/j.jenvman.2021.112438.
Santos, dos.V.F., de Souza, F.J., Duarte, C.A.R. (2016). Reducing bend erosion with a twisted tape insert. Powder Technol. 301, 889–910. https://doi.org/10.1016/j.powtec.2016.07.020.
Scheres, B., Schüttrumpf, H. (2020). Investigating the erosion resistance of different vegetated surfaces for ecological enhancement of sea dikes. J. Mar. Sci. Eng. 8, 519. https://doi.org/10.3390/jmse8070519
Song, J.P., Wang, T., Hu, G.S., Zhang, Z.J., Zhao, W.J., Wang, Z.P., Zhang, Y.G. (2023). Conveying characteristics of shrimp feed pellets in pneumatic conveying system and minimum power consumption dissipation factor. Aquacultural Engineering 102 (10), 2347–2352. https://doi.org/10.1016/j.aquaeng.2023.102347
Stack, M.M., Pungwiwat, N. (2013). Slurry erosion of metallics, polymers, and ceramics: particle size effects. Mater. Sci. Technol. 15, 337–344. https://doi.org/10.1179/026708399101505770
Sun, X.Y., Cao, X.W. (2021). Impact of inter-particle collision on elbow erosion based on DSMC-CFD method. Petrol. Sci. 18, 909-922. https://doi.org/10.1007/s12182-021-00550-5.
Takahashi, K., Tsunoi, S., Hara, T., Ueno, T., Mikami, A., Takada, H., Ando, K., Shiratori, M. (2010). Experimental study of low-cycle fatigue of pipe elbows with local wall thinning and life estimation using finite element analysis. Int. J. Pres. Ves. Pip. 87 (5), 211–219. https://doi.org/10.1016/j.ijpvp.2010.03.022.
Tarodiya, R., Khullar, S., Levy, A. (2022). Particulate flow and erosion modeling of a Pelton turbine injector using CFD-DEM simulations. Powder Technol. 399, 117168. https://doi.org/10.1016/j.powtec.2022.117168
Tofighian, H., Amani, E., Saffar-Avval, M. (2020). A large eddy simulation study of cyclones: the effect of sub-models on efficiency and erosion prediction. Powder Technol. 360, 1237-1252. https://doi.org/10.1016/j.powtec.2019.10.091.
Vieira, R.E., Kesana, N.R., McLaury, B.S., Shirazi, S.A., Torres, C.F., Schleicher, E., Hampel, U. (2014). Experimental investigation of the effect of 90◦ standard elbow on horizontal gas-liquid stratified and annular flow characteristics using dual wire-mesh sensors. Exp. Therm. Fluid Sci. 59, 72–87. https://doi.org/10.1016/j.expthermflusci.2014.08.001.
Wang, B., Guo, H.Y., Geng, X.H., Du, S.N., Zhang, H.J., Wang, W.Q. (2020). Erosion simulation of gas-soild mixed flow in a bent pipe. Journal of Beijing University of Chemical Technology (natural Science) 47 (1), 46–52. https://doi.org/10.13543/j.bhxbzr.2020.01.008
Wang, S., Shi, J., Han, X., Zhu, L., Bi, J., Wang, J., Wang, S., Ma, Z., Wang, Z. (2022). Effect of pipe orientation on erosion of π-shaped pipelines. Powder Technol. 408, 117769. https://doi.org/10.1016/j.powtec.2022.117769
Wang, X., Gong, L., Li, Y., Yao, J. (2023). Developments and applications of the CFD-DEM method in particle–fluid numerical simulation in petroleum engineering: a review. Appl. Therm. Eng. 222, 119865. https://doi.org/10.1016/j.applthermaleng.2022.119865
Wang, Y., Liu, R.T., Liu, M., Yan, J.J. (2019). Numerical investigation on erosion characteristics of coplanar elbows connection for gas-solid flow. Energy Procedia 158, 5245–5250. https://doi.org/10.1016/j.egypro.2019.01.655
Xiao, F., Luo, M., Kuang, S.B., Zhou, M.M., Jing, J.Q., Li, J.F., Lin, R.N., An, J.C. (2021). Numerical investigation of elbow erosion in the conveying of dry and wet particles. Powder Technology 393, 265–279. https://doi.org/10.1016/j.powtec.2021.07.080
Yi, J., He, S., Wang, Z., et al. (2021). Effect of impact angle on the critical flow velocity for erosion-corrosion of 304 stainless steel in simulated sand-containing sea water. J. Bio. Tribo-Corrosion 7 (3), 1-9. https://doi.org/10.1007/s40735-021-00538-z.
Yu, W., Fede, P., Climent, E., Sanders, S. (2019). Multi-fluid approach for the numerical prediction of wall erosion in an elbow, Powder Technol. 354, 561–583. https://doi.org/10.1016/j.powtec.2019.06.007
Yan, L., Ma, X., Miao, X., Wang, Y., Pang, Y., & Song, X. (2024). Numerical investigation and rapid prediction of the erosion rate of gate valve in gas-solid flow. Powder Technology, 448(2). https://doi.org/10.1016/j.powtec.2024.120285
Yao, L.M., Liu, Y.X., Xiao, Z.M., Chen, Y. (2023). An algorithm combining sedimentation experiments for pipe erosion investigation. Energy 270 (12), 6891–6902. https://doi.org/10.1016/j.energy.2023.126891
Yang, Y., Cheng, Y.F. (2012). Parametric effects on the erosion–corrosion rate and mechanism of carbon steel pipes in oil sands slurry. Wear 276-277, 141–148. https://doi.org/10.1016/j.wear.2011.12.010
Yabuki, A., Matsuwaki, K., Matsumura, M. (1999). Critical impact velocity in the solid particles impact erosion of metallic materials. Wear 233, 468-475. https://doi.org/10.1016/S0043-1648(99)00170-2.
Zang, X.R., Cao, X.W., Zheng, W.W., Zhu, T.X., Lei, Y.G., Huang, J.Y., Chen, Z., Teng, L., Bian, J., Lai, Y.K. (2023). Meniscus inspired flexible superhydrophobic coating with remarkable erosion resistance for pipeline gas transmission. Chemical Engineering Journal 451 (13), 8573–8582. http://dx.doi.org/10.2139/ssrn.4140969
Zeng, D.Z., Zhang, E.B., Ding, Y.Y., Yi, Y.G., Xian, Q.B., Yao, G.J., Zhu, H.J., Shi, T.H. (2018). Investigation of erosion behaviors of sulfur-particle-laden gas flow in an elbow via a CFD-DEM coupling method. Powder Technol. 329, 115–128. https://doi.org/ 10.1016/j.powtec.2018.01.056
Zhao, W., Zou, Y., Matsuda, K., Zou, Z. (2016). Corrosion behavior of reheated CGHAZ of X80 pipeline steel in H2S-containing environments. Mater. Des. 99, 44–56. https://doi.org/10.1016/j.matdes.2016.03.036
Zhao, X., Cao, X., Xie, Z., Cao, H., Wu, C., Bian, J. (2022). Numerical study on the particle erosion of elbows mounted in series in the gas-solid flow. J. Nat. Gas Sci. Eng. 99, 104423. https://doi.org/10.1016/j.jngse.2022.104423.
Zhang, J., McLaury, B.S., Shirazi, S.A. (2018). Modeling sand fines erosion in elbows mounted in series. Wear. 402, 196–206. https://doi.org/ 10.1016/j.wear.2018.02.009
Zhou, H., Zhang, Y., Bai, Y., Zhao, H.J., Lei, Y., Zhu, K.Q., Ding, X. (2021). Study on reducing elbow erosion with swirling flow. Colloids and Surfaces a: Physicochemical and Engineering Aspects 630 (12), 7537–7544. https://doi.org/10.1016/j.colsurfa.2021.127537
Zhu, H., Li, S. (2017). Numerical analysis of mitigating elbow erosion with a rib. Powder Technol. 330, 445–460. https://doi.org/10.1016/j. powtec.2018.02.046.